NANO LETTERS

Letter

pubs.acs.org/NanoLett

Catalytic Reduction of 4-Nitrophenol: A Quantitative Assessment of the Role of Dissolved Oxygen in Determining the Induction Time

Eredzhep Menumerov,[†] Robert A. Hughes,[†] and Svetlana Neretina*[,†,‡]

[†]College of Engineering, University of Notre Dame, Notre Dame, Indiana 46556, United States

[‡]Center for Sustainable Energy at Notre Dame, Notre Dame, Indiana 46556, United States

Supporting Information

ABSTRACT: The reduction of 4-nitrophenol to 4-aminophenol by borohydride is one of the foremost model catalytic reactions because it allows for a straightforward assessment of catalysts using the kinetic parameters extracted from the real-time spectroscopic monitoring of an aqueous solution. Crucial to its standing as a model reaction is a comprehensive mechanistic framework able to explain the entire time evolution of the reaction. While much of this framework is in place, there is still much debate over the cause of the induction period, an initial time interval where no reaction seemingly occurs. Here, we report on the simultaneous monitoring of the spectroscopic signal and the dissolved oxygen content within the aqueous solution. It reveals that the induction period is the time interval required for the level of dissolved oxygen to fall below a critical value that is dependent upon whether Au, Ag, or Pd nanoparticles are used as the catalyst. With this understanding, we are able to exert complete control over the induction period, being able to eliminate it, extend it indefinitely, or even induce multiple induction periods over the course of a single reaction. Moreover, we have determined that the reaction product, 4-aminophenol, in the presence of the same catalyst reacts with dissolved oxygen to form 4-nitrophenolate. The implication of these results is that the induction period relates, not to some activation of the catalyst, but to a time interval where the reaction product is being rapidly transformed back into a reactant by a side reaction.

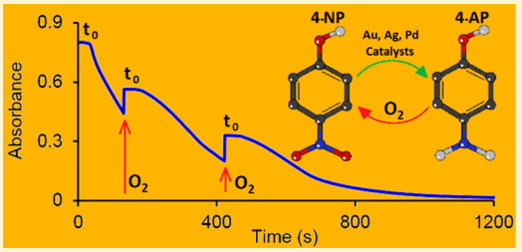

KEYWORDS: *Induction time, delay time, 4-nitrophenol, dissolved oxygen, catalysis, model reaction*

Advancements in heterogeneous catalysis have become increasingly reliant on the placement of chemical controls over nanostructure formation processes that promote atom surface arrangements with the chemical properties needed to optimize catalytic performance. The influence of nanoparticle size, shape, and composition are well-documented[1−3] where increasing emphasis is being placed on obtaining surface atoms with specific coordination environments, promoting beneficial interactions between a catalyst and its support, and minimizing the often detrimental effects of nanostructure capping agents.[4−6] While emphasis has been rightfully placed on these parameters, the highly reactive nature of the resulting catalytic surfaces can lead to unwanted side reactions and make them susceptible to poisoning.[7] Heterogeneous catalysis utilizing metal nanostructures in aqueous solutions containing dissolved oxygen are particularly susceptible to such deleterious effects since they often have a high affinity for oxygen. The interactions between dissolved oxygen and nanostructures have, in fact, been utilized in detection schemes,[8,9] influenced nanostructure growth modes,[10−13] and altered nanostructure aggregation kinetics.[14] Its influence on catalysis is, however, often ignored or minimized by purging aqueous solutions with chemically inert gases, a remedy that is rarely quantified and impractical for some applications.

The reduction of 4-nitrophenol (4-NP) by borohydride on catalytic surfaces has emerged as one of the most widely used model reactions for assessing the catalytic[15,16] and photocatalytic[17−19] properties of nanoscale[16,20−34] and nanostructured bulk[35] materials. Its designation as a model catalytic reaction[15,16] stems from both its simplicity and the ease by which the reaction can be monitored using spectroscopic techniques. The reaction occurs in water under ambient conditions, has no known side reactions, and will only proceed if a catalyst is present. High-precision real-time monitoring is made possible by spectroscopically observing successive reductions in the characteristic absorbance of 4-nitrophenolate ions at 400 nm and a concomitant rise at 300 nm associated with the product of the reaction, 4-aminophenol (4-AP). The reaction, when carried out in excess borohydride, is understood in terms of the Langmuir−Hinshelwood model.[36−38] The reactants, consisting of 4-NP and a surface−hydrogen species derived from borohydride, are first adsorbed onto the surface of the catalyst, a process that is rapid, reversible, and described in terms of Langmuir isotherms.[36] After an induction period, where no reaction seemingly occurs, a pseudo-first-order reaction proceeds yielding 4-AP, a species that rapidly desorbs from the surface and is, hence, inconsequential to the reaction kinetics. The rate-limiting step is, therefore, the reaction

Received: September 23, 2016
Revised: November 21, 2016
Published: November 28, 2016

DOI: 10.1021/acs.nanolett.6b03991
Nano Lett. 2016, 16, 7791−7797

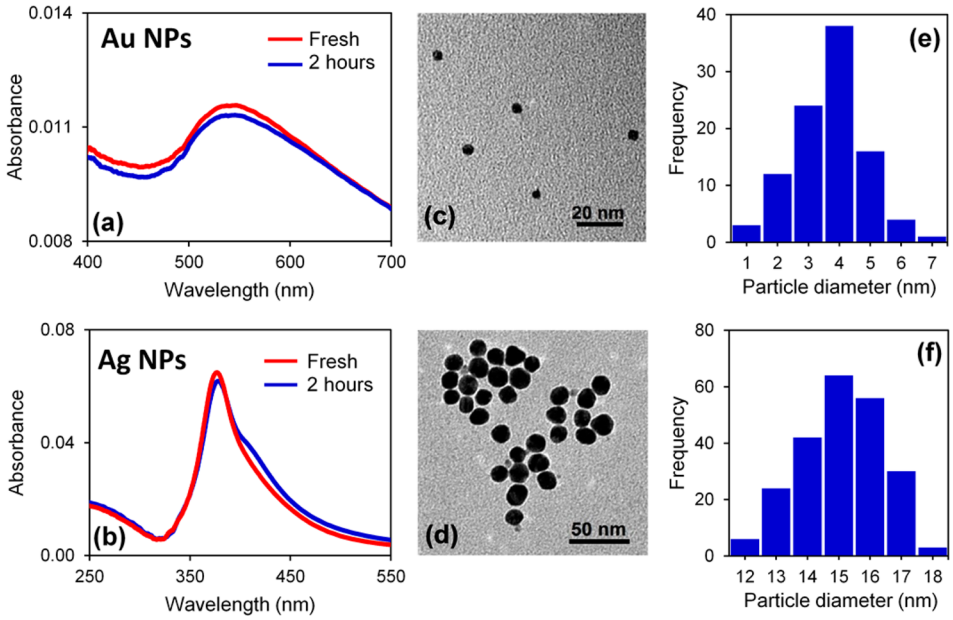

Figure 1. Absorbance spectrum of (a) Au and (b) Ag nanoparticles showing the LSPR peak obtained immediately after synthesis and again after 2 h. TEM images and histograms of the nanoparticle size distribution for the (c,e) Au and (d,f) Ag nanoparticles.

occurring between the adsorbed hydrogen species and 4-NP on the metal catalyst. Catalysts are typically described in terms of an apparent reaction rate constant, k_{app}, equal to the linear slope of the $\ln(A/A_0)$ vs time plot, where A/A_0 is the 4-NP absorbance normalized to its value at the end of the induction period.[15] The temperature dependence of k_{app} follows Arrhenius behavior[15,39] and can, hence, be used to determine the activation energy for the reaction.

While the current understanding of the catalytic reduction of 4-NP by borohydride affords a full analysis of the temperature-dependent reaction kinetics,[36,37,40] the origin of the induction period remains somewhat of an enigma. Early work demonstrated that the induction period could be significantly reduced or even eliminated for Ag nanoparticles if a N_2 gas purge is used to rid the reactants of dissolved oxygen, a result that led the authors to conclude that the induction period is the time required for borohydride to dissolve an oxide layer that poisoned an otherwise catalytic surface.[41] This explanation, however, proved unsatisfactory when induction times were also observed for nanoparticles of nonoxidizable metals (e.g., Au, Pt).[37,42,43] Ballauff and co-workers initially suggested that dissolved oxygen outcompetes 4-NP for borohydride, and as a result, the reaction could only initiate once all of the dissolved oxygen was consumed.[42,44] More recently, the same group began to advocate an alternate explanation in which the reaction could only begin once the catalyst surface underwent a surface reconstruction brought on by the attachment of reactants to the surface.[36] Their proposed mechanism for catalyst activation was supported by kinetic arguments as well as the corroborative work by Chen and co-workers[45,46] who came to a similar conclusion for the catalytic reduction of resazurin by NH_2OH. An irreversible surface reconstruction also accounted for the fact that no induction period is observed when their catalyst is reused.[47] This explanation has received considerable support[47−49] but also has its detractors who argue that reused catalysts can, in fact, have an induction period[50,51] and that photoluminescence spectra taken before and after the reaction show no indication that the nanoparticles have undergone a reconstruction.[52] Even the proponents of this mechanism concede that no structural evidence exists in support of a surface reconstruction.[15] Zeng et al.,[53] in a study that showed the exceptional catalytic activity realizable from Au-based nanocages, suggested that the induction period was the time required for 4-NP attachment to the catalyst surface. Ballauff and co-workers have, however, forwarded opposing arguments, based on an estimate of the Damköhler number ($DaII$), that indicate that the reaction is limited, not by the diffusion of reactants to the catalyst, but by the kinetics of the reaction occurring on the catalyst surface.[36] Others have argued both in favor[43,50,52,54−56] and in opposition[48] to such a diffusion-limited mechanism, a discussion that is complicated by the varied nature of catalyst supports and surface ligands and their potential impact on the diffusion of reactants to catalytically active sites. Another proposed mechanism attributes the induction period to the time required for borohydride ions to inject electrons into the catalyst, where the resulting increase in the Fermi energy lowers the reduction potential of the reaction to the extent that it allows the reaction to proceed.[57,58] The overall state of the literature is, hence, one where there exists no consensus and where irrefutable experimental evidence for any proposed mechanism is lacking.

An examination of the literature also reveals that, while it is recognized that dissolved oxygen can influence the catalytic reduction of 4-NP, an in-depth understanding does not yet exist. In fact, many researchers routinely purge the reactants with N_2 or Ar gas in an attempt to rid the experimental system of dissolved oxygen and, hence, avoid these complicating factors. With issues involving dissolved oxygen left unreconciled, we initiated a study in which we spectroscopically monitored the reduction of 4-NP by borohydride using Au, Ag, and Pd nanoparticles while simultaneously carrying out an in situ measurement of the dissolved oxygen content. By purging the reactants with either O_2 or Ar gas, we were able to systematically vary the dissolved oxygen content and, hence, obtain a quantitative assessment of its influence on the reaction. Here, we show that dissolved oxygen is the decisive factor in

DOI: 10.1021/acs.nanolett.6b03991
Nano Lett. 2016, 16, 7791−7797

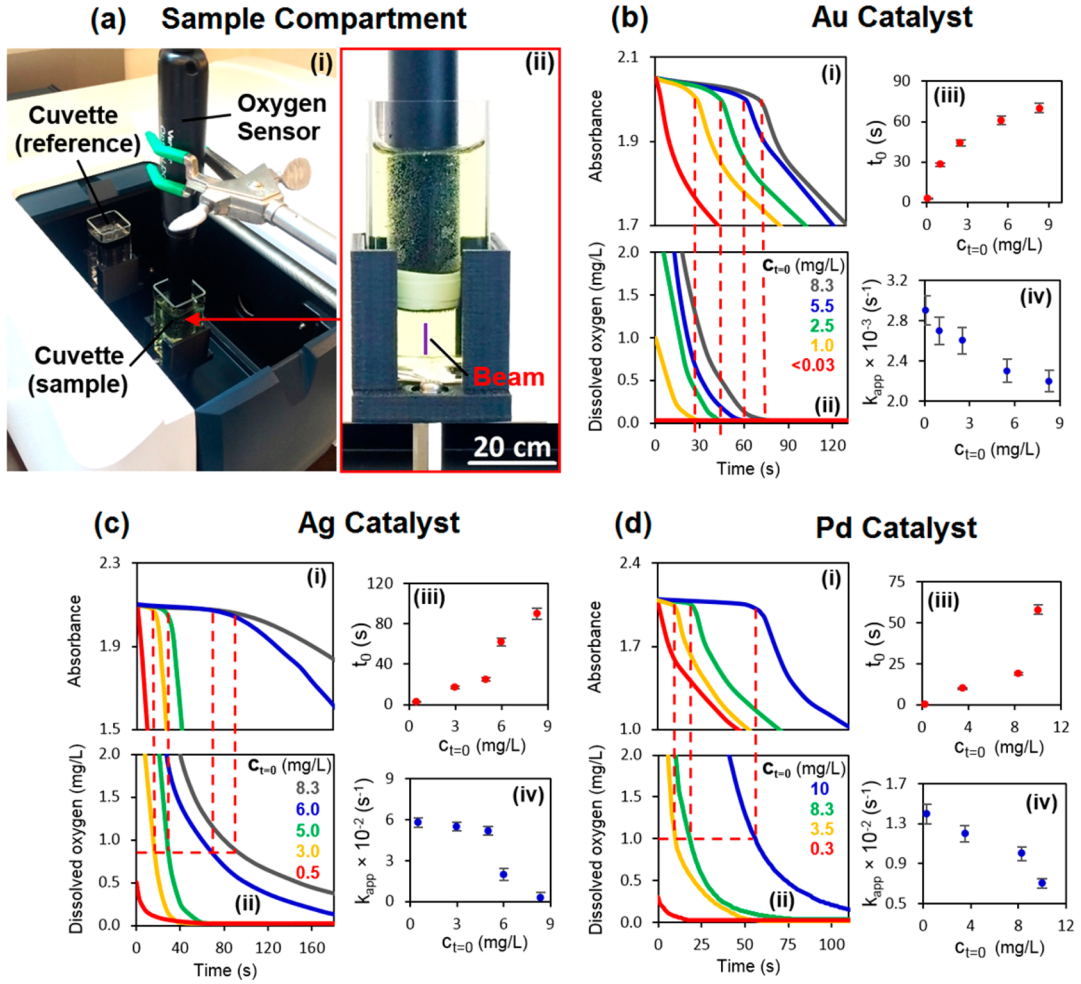

Figure 2. (a) Image of (i) the sample compartment of the UV−vis spectrometer that has been modified to accommodate two 2.5 cm path length cuvettes and a dissolved oxygen sensor and (ii) a magnified view of the sensor when submerged in a partially reacted 4-NP solution. The time-dependent (i) absorbance and (ii) dissolved oxygen concentration as $c_{t=0}$ is systematically varied for (b) Au, (c) Ag, and (d) Pd catalysts. Extracted from the absorbance data for each catalyst is the dependence of the (iii) induction time (t_0) and (iv) apparent rate constant (k_{app}) on $c_{t=0}$.

determining the induction time. Real-time monitoring indicates, not only the consumption of dissolved oxygen, but also an induction period that ends when a critical value for the dissolved oxygen content is achieved, a value that is dependent on the catalyst material. Based on these results we present a mechanistic framework able to rationalize our results both self-consistently and within the context of the preceding literature.

Colloidal nanoparticles of Au, Ag, and Pd were formed using a room temperature aqueous synthesis in which metal ions derived from $HAuCl_4$, $AgNO_3$, and $Pd(NO_3)_2$ were reduced with $NaBH_4$ (see Supporting Information for details). The synthesis closely follows the protocol set forth by Deraedt et al.[59] who demonstrated the long-term stability of Au nanoparticles produced by this method as well as exceptional catalytic activity toward the reduction of 4-NP by borohydride. Our synthesis, however, differs in that a series of measures were taken to rid the solution of dissolved oxygen (vide infra). The ability to form stabilized colloidal nanoparticles using $NaBH_4$, the same reducing agent as that used in 4-NP catalysis, simplifies this mechanistic study in that potential complications arising from the use of sophisticated ligands or supports are negated. The stability of the Au and Ag nanoparticles were confirmed using UV−vis spectroscopy. Figure 1a,b shows that the localized surface plasmon resonances (LSPR) remains essentially unchanged over a 2 h period. This "window" of stability allowed for multiple catalysis measurements using the same stock solution. A similar confirmation could not be made for Pd nanoparticles because no measurable LSPR was observed. In an effort to mitigate possible aging effects, reactions involving Pd catalysts utilized freshly prepared nanoparticles. It is also noted that the catalytic properties of Pd, as well as the conclusions drawn, are consistent with those obtained using Au and Ag nanoparticles. Transmission electron microscope (TEM) images and histograms of the nanoparticle size distributions are shown in Figure 1c−f and Figure S3 of Supporting Information.

Critical to this study is the capability to spectroscopically monitor the reduction of 4-NP while simultaneously carrying out an in situ measurement of the dissolved oxygen content within the aqueous solution. While statements appear in the literature regarding the influence of dissolved oxygen on this reaction, we are unaware of any prior work where a measurement of this quantity has occurred at any stage of the reaction. Real-time monitoring required that modifications be made to the sample compartment of the spectrometer (Figure 2a) that allow for the use of a cuvette that is large enough (vol. 38 mL, path length 2.5 cm) to accommodate the physical dimensions of the oxygen sensor. Control experiments

DOI: 10.1021/acs.nanolett.6b03991
Nano Lett. 2016, 16, 7791−7797

indicate that the measured induction times and rate constants are unperturbed by the presence of this sensor and that its readings are unaffected by the evolving H_2 gas from borohydride hydrolysis (Supporting Information, Figure S4). The dissolved oxygen content was varied by purging the starting solution of aqueous 4-NP with Ar gas where increased purging times yielded lower values. In some instances, the dissolved oxygen content was raised by purging with O_2 gas. While varying the dissolved oxygen content is a relatively straightforward process, stringent procedures are required for it to be reduced from an ambient value of 8.3 mg·L^{-1} to levels below the detection limit of the sensor (i.e., 0.03 mg·L^{-1}), levels that we show to be of consequence to the catalytic reduction of 4-NP. To obtain such low values requires that all reactant-containing solutions (i.e., catalyst, 4-NP, $NaBH_4$) be purged and that exposed liquid surfaces be kept under Ar. Exposing the surface of 8 mL of deaerated aqueous 4-NP to air, for example, shows a more than 10-fold increase in the dissolved oxygen content in under 3 min (Supporting Information, Figure S5a). If these same measurements were to have occurred in a standard 3.5 mL cuvette with a 1 cm path length, then the dissolved oxygen levels would have been even greater because the surface area exposed to air per unit volume of liquid would have been approximately 3× larger. The uptake of dissolved oxygen is also impacted by any stirring or turbulence created when one solution is pipetted into another under air exposure. Based on our cumulative experience, we strongly suspect that few, if any, studies have taken the precautions necessary to purge the dissolved oxygen to levels where they have no impact on 4-NP reduction.

Catalysis measurements were carried out using 4-NP and borohydride concentrations of 50 μM and 5 mM, respectively. The 4-NP concentration was chosen to be about half the value that is typically used in order to offset the greater attenuation of the beam resulting from the cuvette's 2.5 cm path length. The larger cuvette volume, however, results in the reduction of 4× as many 4-NP molecules then is typical. It is also noted that, at the ambient concentration, the number of dissolved oxygen molecules outnumber 4-NP molecules by a factor of 1.7. Reactants were pipetted into the cuvette in the sequence (i) 4-NP, (ii) borohydride, and (iii) catalyst where efforts were made to promote consistent timing for all reactions so as to promote fair comparisons. Figure 2b–d shows the temporal dependence of both the absorbance at 400 nm (i.e., the 4-nitrophenolate peak position) and the dissolved oxygen concentration for Au, Ag, and Pd catalysts where each curve represents a different dissolved oxygen concentration at t = 0 s. The absorbance is only shown near the beginning of the reaction so as to highlight changes to the induction time (see Figures S6–S8 of Supporting Information for the complete data set). Accompanying these dependencies are the extracted values for the induction time (t_0) and the apparent rate constant (k_{app}) as a function of the dissolved oxygen content in the 4-NP solution at t = 0 s (denoted as $c_{t=0}$).

For all cases, the onset of the reaction is accompanied by a precipitous fall in the dissolved oxygen concentration to levels below the detection limit, confirming that dissolved oxygen is consumed in the reaction. The data also show a strong correlation between t_0 and $c_{t=0}$, indicating that shorter duration induction times occur when less dissolved oxygen is present at the beginning of the reaction. For all three catalysts the induction period is eliminated when $c_{t=0}$ is sufficiently reduced, where the Au catalyst requires the largest reduction and Pd requires the smallest. An examination of the dissolved oxygen content occurring at the end of each induction period (denoted by red dashed lines) reveals that there exists a critical value (c_{CR}) for each catalyst, below which the reduction of 4-NP is observed. The critical value for Ag and Pd occurs at 0.8 and 1 mg·L^{-1}, respectively, while for Au it is just below the detection limit. The induction time is, hence, the time required for the dissolved oxygen content to fall below a critical value. If the dissolved oxygen concentration is below c_{CR} at t = 0 s then the induction period is absent from the reaction. It should be recognized, however, that the reported c_{CR} values are unique to the set of reaction conditions used and will inevitably have dependencies on the reactant concentrations, the type and amount of catalyst used, the temperature at which the reaction is carried out, etc. It is, for example, shown as Supporting Information (Figures S9–S11), that while variations to c_{CR}, k_{app}, and t_o occur as the nanoparticle size is varied, the influence of dissolved oxygen on these quantities follows the same tendencies as those described herein, an indication that these tendencies are universal rather than being unique to specific nanostructures. The Au, Ag, and Pd catalysts also show an increase in k_{app} as $c_{t=0}$ is reduced to values below the detection limit, with Au and Pd showing only a slight increase and Ag showing an impressive 20-fold increase. The result indicates that dissolved oxygen is inhibitory toward the reduction of 4-NP, but to a degree that is strongly dependent on the catalyst used.

The consumption of dissolved oxygen during the catalytic reduction of 4-NP has been previously proposed,[42,54] but experimental verification has not occurred. The loss of dissolved oxygen is thought to occur through borohydride oxidation according to[60]

$$BH_4^- + 2O_2 + H^+ \rightarrow H_3BO_3 + H_2O \quad (1)$$

In an effort to assess this reaction and determine whether the various catalysts influence it, the dissolved oxygen content was monitored for aqueous solutions containing 4-NP (8 mL, 150 μM) with an initial dissolved oxygen concentration of 8.3 mg·L^{-1} into which $NaBH_4$ (8 mL, 15 mM) and (i) Au, (ii) Ag, and (iii) Pd nanoparticles (8 mL, 5 μM) are added (Figure 3a). A fourth reaction in which the catalyst solution was replaced with deaerated water was also monitored. The results reveal that borohydride, as expected, consumes dissolved oxygen, but where the reaction rate is enhanced in the presence of a catalyst. The Au catalyst gives rise to the largest enhancement, while Ag results in the smallest. The catalytic reduction of 4-NP, hence, involves one reactant where the dissolved oxygen content is stable (i.e., 4-NP), a second where it is consumed (i.e., $NaBH_4$), and a catalyst which, when combined with $NaBH_4$, enhances the rate of oxygen consumption to a degree that is dependent upon the catalyst material. The implication of these results on the reduction of 4-NP is that there exists a steadily changing dissolved oxygen content that impacts, not only the kinetic parameters, but also the values obtained for these parameters when variations occur to the sequence and timing in which these reactants are combined.

In addition to the consumption of dissolved oxygen, the catalytic reduction of 4-NP is also accompanied by the evolution of H_2 gas originating from the hydrolysis of borohydride.[40] In an effort to quantify this reaction we monitored the volume of gas evolving from a 24 mL solution containing the same reactant concentrations and volumes as used in the catalysis measurements (Figure 3b). The data

DOI: 10.1021/acs.nanolett.6b03991
Nano Lett. 2016, 16, 7791–7797

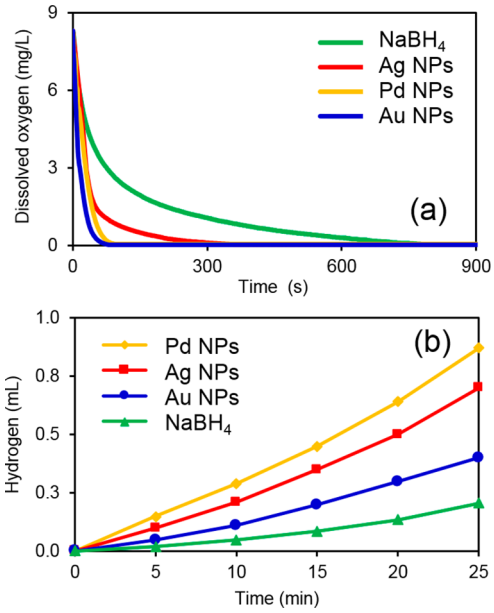

Figure 3. (a) Time evolution of the dissolved oxygen content of water into which borohydride and the various catalysts are added. (b) The cumulative volume of the H_2 gas released from a 24 mL solution containing 4-NP and $NaBH_4$ and identical solutions into which 5 μM of catalysts are added.

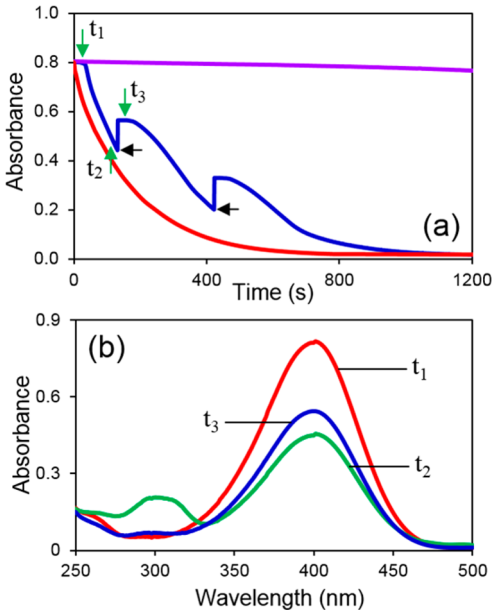

Figure 4. (a) Time-dependent absorbance at 400 nm as the Au nanoparticles catalyze the reduction of 4-NP using reactants where dissolved oxygen is (i) removed (red), (ii) continuously replenished through an O_2 gas purge (violet), and (iii) replenished through two 5 s O_2 gas purges initiated at the times denoted by black arrows (blue). (b) The absorbance spectra for an identical reaction taken at times t_1, t_2, and t_3 (denoted by green arrows in Figure 4a).

indicates that the rate at which gas is released is enhanced in the presence of a catalyst where Pd offers the largest enhancement and Au the least. While it is tempting to associate H_2 gas generation with the rate at which the hydrogen species required for 4-NP reduction is produced, such an assignment cannot be definitively made. It is, however, noteworthy that the hierarchy in c_{CR} values for the three catalysts follows the same trend as that observed for H_2 generation. It should also be recognized that any self-purging of dissolved oxygen by the evolving H_2 gas is expected to be minimal since the efficient removal of dissolved oxygen requires that Ar be bubbled through the reactants at a flow rate that is approximately 5000× greater than the H_2 gas generated from the reaction.

In further support of our claim that dissolved oxygen is responsible for the induction period, we carried out reactions using an Au catalyst in which O_2 gas was bubbled through the reactants as the 4-NP absorbance was continuously monitored. This O_2 gas purge, hence, provides the means to replenish dissolved oxygen as it is consumed. Figure 4a shows the time-dependent absorbance for reactions where (i) the dissolved oxygen is reduced to values below the detection limit, (ii) O_2 gas is continuously bubbled through the reactants, and (iii) O_2 gas is bubbled through the reactants for two 5 s intervals occurring partway through the reaction. The data reveals that, while a sufficient reduction in the dissolved oxygen content eliminates the induction period, continuous replenishment extends it indefinitely. The dissolved oxygen obtained during the 5 s O_2 gas purges, while temporarily stalling the reaction, is unable to maintain this condition once it too is consumed. With the capability to eliminate, extend, or induce multiple induction periods through the manipulation of the dissolved oxygen content, it is difficult to refute that a mechanistic connection exists between the dissolved oxygen content and the induction period.

It is also revealing that the two 5 s O_2 gas purges result, not only in multiple induction periods, but also in a sudden rise in the absorbance. The result suggests that additional 4-nitrophenolate is created when dissolved oxygen is added. Confirmation was obtained by monitoring the entire spectrum instead of just the 400 nm wavelength. Figure 4b shows the spectra obtained at the beginning of the reaction (t_1), just prior to the addition of oxygen (t_2), and immediately after the first 5 s O_2 gas purge (t_3). The data indicates that the O_2 purge leads to an increase in the 4-NP peak as well as a decrease in the 4-AP peak. The implication of this result is that a side reaction occurs in which 4-aminophenol (or 4-aminophenolate) reacts with dissolved oxygen to form 4-nitrophenolate. It is noted that control experiments in which 5 s Ar purges were used instead of O_2 saw no sudden rise in the 4-NP absorbance (Supporting Information, Figure S12), further confirming that dissolved oxygen is solely responsible for the observed behavior.

With the discovery of a side reaction capable of converting 4-AP into 4-NP in the presence of dissolved oxygen, it becomes possible to explain the induction period if it is assumed that the kinetics of this side reaction are significantly faster than those associated with 4-NP reduction. In such a scenario, the catalytic reduction of 4-NP occurs throughout the induction period, but where the reaction is undetectable because the 4-AP produced is rapidly transformed back into 4-NP by the side reaction. The ability of this side reaction to work in opposition to the main reaction will, however, be degraded as the dissolved oxygen is exhausted through a reaction with borohydride. In the absence of the side reaction, the 4-NP levels fall as it is reduced to 4-AP. Thus, a reaction that was occurring all along transforms from one that is spectroscopically undetectable to one that is detectable. If this explanation is correct, then it not only accounts for the induction period, but it also eliminates the need for a mechanism able to activate the catalyst since it is active at t = 0 s.

DOI: 10.1021/acs.nanolett.6b03991
Nano Lett. 2016, 16, 7791−7797

An understanding of the critical oxygen concentration is somewhat more involved. It occurs at the dissolved oxygen concentration where the rate at which 4-AP is produced exceeds the rate at which 4-AP is converted back to 4-NP by the side reaction. While this requirement is straightforward, it should be recognized that at least four reactions are occurring during the induction period: (i) the reduction of 4-NP to 4-AP, (ii) the consumption of oxygen by borohydride, (iii) the hydrolysis of borohydride, and (iv) the transformation of 4-AP back into 4-NP by the side reaction. These reactions do not occur in isolation, but are instead highly intertwined with reactants and products of certain reactions being reactants for other reactions. With at least three of these reactions being catalytically driven there is also a competition for active sites whose effectiveness for any given reaction is dependent on numerous factors including the reactant concentrations and the type, size, faceting, and amount of catalyst used. Despite this complexity, we note that the hierarchy in c_{CR} values for the three catalysts studied follows the same trend as that observed for H_2 generation. If, as previously suggested, the rate of H_2 gas generation provides a measure of the rate at which the hydrogen species required for 4-NP reduction is produced, then it would account for the fact that c_{CR} increases for catalysts generating greater quantities of H_2 gas because the generation of the hydrogen species in greater quantities facilitates higher rates of 4-NP reduction to 4-AP (i.e., the stated requirement for higher c_{CR} values).

The findings and understanding garnered from this study can be reconciled with much of the preceding 4-NP literature. The sensitivity of the induction time to dissolved oxygen[41,42,44] has been confirmed and explained. The meticulous kinetic studies carried out by Wunder et al.[36,37] using Au nanoparticles have demonstrated a close, yet unexplained, connection between the kinetics governing the induction period and those associated with the catalytic reduction of 4-NP, with both k_{app} and t_0 showing nearly identical activation energies. This observation can now be understood since the catalytic reduction of 4-NP occurs both during and after the induction period, where in both cases it represents the rate-limiting step. While the occurrence of a side reaction may seem problematic in terms of describing 4-NP reduction as a pseudo-first-order reaction, it is, in fact, the expected result for the Au catalyst since the side reaction nears completion before 4-NP reduction becomes measurable. Deviations from first-order behavior are, however, expected for catalysts with higher values of c_{CR} because dissolved oxygen is still being consumed by the side reaction for times extending beyond the induction period. In these instances, one would expect a rounding in the absorbance near the induction time and a reaction rate that appears to increase as the influence of the opposing side reaction diminishes, effects that are pronounced in our Ag catalyst absorbance data (Supporting Information, Figure S7) as well those of others.[44,47] The sensitivity of the induction period to the order in which reactants are added[39,43,61,62] can also be understood since an earlier addition of aqueous borohydride initiates oxygen consumption, while a later addition postpones it. We also suspect that reports of severe reductions to the induction time when reusing catalysts[41,47,49,52] originate from the use of previously reacted solutions in which the dissolved oxygen content was drastically reduced. We, however, concede that it is often difficult to make such a determination since many of these reports lack sufficient experimental detail. On a similar note, we cannot, given the diverse collection of the catalysts, surface ligands, and supports that comprise the 4-NP literature, rule out the possibility that other proposed mechanisms could also give rise to an induction period. We, however, contend that there is no reason to invoke such a mechanism until dissolved oxygen has been fully ruled out as the cause.

In summary, we have carried out a quantitative assessment of the role of dissolved oxygen in the catalytic reduction of 4-NP by borohydride. By employing an experimental configuration that allows for the simultaneous real-time monitoring of the 4-NP absorbance and the dissolved oxygen concentration, it has been determined that the induction period ends once the level of dissolved oxygen falls below a critical value that is dependent upon the catalyst used. If the starting reactants contain a dissolved oxygen concentration that lies below this value, then the induction period is absent from the reaction. It is further shown that an ongoing reaction can be halted if the dissolved oxygen is replenished through an O_2 gas purge, a process that is accompanied by the formation of 4-NP. Based on these findings, we conclude that the induction period is caused by the rapid conversion of 4-AP (or 4-aminophenolate) back into 4-nitrophenolate by a side reaction that terminates when the dissolved oxygen is consumed. This study has, hence, further defined the mechanistic constructs needed to fully understand an important model catalytic reaction and has established the procedures needed to eliminate dissolved oxygen as a confounding factor when assessing catalytic materials.

■ ASSOCIATED CONTENT

Supporting Information

The Supporting Information is available free of charge on the ACS Publications website at DOI: 10.1021/acs.nanolett.6b03991.

Experimental details and additional data (PDF)

■ AUTHOR INFORMATION

Corresponding Author

*E-mail: sneretina@nd.edu (S.N.).

ORCID

Svetlana Neretina: 0000-0002-6889-4384

Notes

The authors declare no competing financial interest.

■ ACKNOWLEDGMENTS

This work is supported by a National Science Foundation Award (DMR-1505114) to S.N. The authors are grateful to M. F. Repetto (Department of Biology, Temple University) for the advice provided in terms of the use and selection of a dissolved oxygen sensor. The work has benefited from the facilities available through the Notre Dame Integrated Imaging Facility (NDIIF) and the expertise of S. Rouvimov (Transmission Electron Microscopy Program Director).

■ REFERENCES

(1) Ruditskiy, A.; Peng, H.-C.; Xia, Y. *Annu. Rev. Chem. Biomol. Eng.* **2016**, *7*, 327−348.
(2) Cao, S.; Tao, F.; Tang, Y.; Li, Y.; Yu, J. *Chem. Soc. Rev.* **2016**, *45*, 4747−4765.
(3) Zaera, F. *ChemSusChem* **2013**, *6*, 1797−1820.
(4) Jenkins, S. V.; Chen, S.; Chen, J. *Tetrahedron Lett.* **2015**, *56*, 3368−3372.

DOI: 10.1021/acs.nanolett.6b03991
Nano Lett. 2016, 16, 7791−7797

(5) Ciganda, R.; Li, N.; Deraedt, C.; Gatard, S.; Zhao, P.; Salmon, L.; Hernández, R.; Ruiz, J.; Astruc, D. *Chem. Commun.* **2014**, *50*, 10126−10129.
(6) Li, D.; Wang, C.; Tripkovic, D.; Sun, S.; Markovic, N. M.; Stamenkovic, V. R. *ACS Catal.* **2012**, *2*, 1358−1362.
(7) Argyle, M. D.; Bartholomew, C. H. *Catalysts* **2015**, *5*, 145−269.
(8) Zhang, Z.; Chen, Z.; Cheng, F.; Zhang, Y.; Chen, L. *Analyst* **2016**, *141*, 2955−2961.
(9) Song, Y. Z.; Song, W.; Qian, L.; Wang, J. H.; Zhang, X. M.; Lu, X.; Xie, J. *Int. J. Electrochem. Sci.* **2014**, *9*, 6843−6851.
(10) Long, R.; Zhou, S.; Wiley, B. J.; Xiong, Y. *Chem. Soc. Rev.* **2014**, *43*, 6288−6310.
(11) Wu, X.; Redmond, P. L.; Liu, H.; Chen, Y.; Steigerwald, M.; Brus, L. *J. Am. Chem. Soc.* **2008**, *130*, 9500−9506.
(12) Callegari, A.; Tonti, D.; Chergui, M. *Nano Lett.* **2003**, *3*, 1565−1568.
(13) Sui, Y.; Fu, W.; Zeng, Y.; Yang, H.; Zhang, Y.; Chen, H.; Li, Y.; Li, M.; Zou, G. *Angew. Chem., Int. Ed.* **2010**, *49*, 4282−4285.
(14) Zhang, W.; Yao, Y.; Li, K.; Huang, Y.; Chen, Y. *Environ. Pollut.* **2011**, *159*, 3757−3762.
(15) Hervés, P.; Pérez-Lorenzo, M.; Liz-Marzán, L. M.; Dzubiella, J.; Lu, Y.; Ballauff, M. *Chem. Soc. Rev.* **2012**, *41*, 5577−5587.
(16) Zhao, P.; Feng, X.; Huang, D.; Yang, G.; Astruc, D. *Coord. Chem. Rev.* **2015**, *287*, 114−136.
(17) Hajfathalian, M.; Gilroy, K. D.; Yaghoubzade, A.; Sundar, A.; Tan, T.; Hughes, R. A.; Neretina, S. *J. Phys. Chem. C* **2015**, *119*, 17308−17315.
(18) Liu, Y.; Tang, A.; Zhang, Q.; Yin, Y. *J. Am. Chem. Soc.* **2015**, *137*, 11327−11339.
(19) Gao, S.; Zhang, Z.; Liu, K.; Dong, B. *Appl. Catal., B* **2016**, *188*, 245−252.
(20) Li, J.; Sun, X.; Qin, D. *ChemNanoMat* **2016**, *2*, 494−499.
(21) Ye, H.; Wang, Q.; Catalano, M.; Lu, N.; Vermeylen, J.; Kim, M. J.; Liu, Y.; Sun, Y.; Xia, X. *Nano Lett.* **2016**, *16*, 2812−2817.
(22) Zhang, S.; Chang, C.-R.; Huang, Z.-Q.; Li, J.; Wu, Z.; Ma, Y.; Zhang, Z.; Wang, Y.; Qu, Y. *J. Am. Chem. Soc.* **2016**, *138*, 2629−2637.
(23) Thota, S.; Chen, S.; Zhao, J. *Chem. Commun.* **2016**, *52*, 5593−5596.
(24) Wang, C.; Salmon, L.; Li, Q.; Igartua, M. E.; Moya, S.; Ciganda, R.; Ruiz, J.; Astruc, D. *Inorg. Chem.* **2016**, *55*, 6776−6780.
(25) Roy, A.; Debnath, B.; Sahoo, R.; Chandrakumar, K. R. S.; Ray, C.; Jana, J.; Pal, T. *J. Phys. Chem. C* **2016**, *120*, 5457−5467.
(26) Bae, S.; Gim, S.; Kim, H.; Hanna, K. *Appl. Catal., B* **2016**, *182*, 541−549.
(27) Soetan, N.; Zarick, H. F.; Banks, C.; Webb, J. A.; Libson, G.; Coppola, A.; Bardhan, R. *J. Phys. Chem. C* **2016**, *120*, 10320−10327.
(28) Kästner, C.; Thünemann, A. F. *Langmuir* **2016**, *32*, 7383−7391.
(29) Quast, A. D.; Bornstein, M.; Greydanus, B. J.; Zharov, I.; Shumaker-Parry, J. S. *ACS Catal.* **2016**, *6*, 4729−4738.
(30) Sun, X.; Qin, D. *J. Mater. Chem. C* **2015**, *3*, 11833−11841.
(31) Gong, M.; Jin, X.; Sakidja, R.; Ren, S. *Nano Lett.* **2015**, *15*, 8347−8353.
(32) Gu, S.; Kaiser, J.; Marzun, G.; Ott, A.; Lu, Y.; Ballauff, M.; Zaccone, A.; Barcikowski, S.; Wagener, P. *Catal. Lett.* **2015**, *145*, 1105−1112.
(33) Zhang, J.; Chen, G.; Guay, D.; Chaker, M.; Ma, D. *Nanoscale* **2014**, *6*, 2125−2130.
(34) Chen, S.; Jenkins, S. V.; Tao, J.; Zhu, Y.; Chen, J. *J. Phys. Chem. C* **2013**, *117*, 8924−8932.
(35) Menumerov, E.; Gilroy, K. D.; Hajfathalian, M.; Murphy, C. J.; McKenzie, E. R.; Hughes, R. A.; Neretina, S. *Catal. Sci. Technol.* **2016**, *6*, 5737−5745.
(36) Wunder, S.; Lu, Y.; Albrecht, M.; Ballauff, M. *ACS Catal.* **2011**, *1*, 908−916.
(37) Wunder, S.; Polzer, F.; Lu, Y.; Mei, Y.; Ballauff, M. *J. Phys. Chem. C* **2010**, *114*, 8814−8820.
(38) Antonels, N. C.; Meijboom, R. *Langmuir* **2013**, *29*, 13433−13442.
(39) Nemanashi, M.; Meijboom, R. *J. Colloid Interface Sci.* **2013**, *389*, 260−267.
(40) Gu, S.; Wunder, S.; Lu, Y.; Ballauff, M. *J. Phys. Chem. C* **2014**, *118*, 18618−18625.
(41) Pradhan, N.; Pal, A.; Pal, T. *Colloids Surf., A* **2002**, *196*, 247−257.
(42) Mei, Y.; Lu, Y.; Polzer, F.; Ballauff, M. *Chem. Mater.* **2007**, *19*, 1062−1069.
(43) Kalekar, A. M.; Sharma, K. K. K.; Lehoux, A.; Audonnet, F.; Remita, H.; Saha, A.; Sharma, G. K. *Langmuir* **2013**, *29*, 11431−11439.
(44) Lu, Y.; Mei, Y.; Walker, R.; Ballauff, M.; Drechsler, M. *Polymer* **2006**, *47*, 4985−4995.
(45) Zhou, X.; Xu, W.; Liu, G.; Panda, D.; Chen, P. *J. Am. Chem. Soc.* **2010**, *132*, 138−146.
(46) Xu, W.; Kong, J. S.; Yeh, Y.-T. E.; Chen, P. *Nat. Mater.* **2008**, *7*, 992−996.
(47) Mei, Y.; Sharma, G.; Lu, Y.; Ballauff, M.; Drechsler, M.; Irrgang, T.; Kempe, R. *Langmuir* **2005**, *21*, 12229−12234.
(48) Ansar, S. M.; Kitchens, C. L. *ACS Catal.* **2016**, *6*, 5553−5560.
(49) Nigra, M. M.; Ha, J. M.; Katz, A. *Catal. Sci. Technol.* **2013**, *3*, 2976−2983.
(50) Zhang, M.; Bacik, D. B.; Roberts, C. B.; Zhao, D. *Water Res.* **2013**, *47*, 3706−3715.
(51) Torkamani, F.; Azizian, S. *J. Mol. Liq.* **2016**, *214*, 270−275.
(52) Yamamoto, H.; Yano, H.; Kouchi, H.; Obora, Y.; Arakawa, R.; Kawasaki, H. *Nanoscale* **2012**, *4*, 4148−4154.
(53) Zeng, J.; Zhang, Q.; Chen, J.; Xia, Y. *Nano Lett.* **2010**, *10*, 30−35.
(54) Lu, P.; Campbell, C. T.; Xia, Y. *Nano Lett.* **2013**, *13*, 4957−4962.
(55) Signori, A. M.; Santos, K. d. O.; Eising, R.; Albuquerque, B. L.; Giacomelli, F. C.; Domingos, J. B. *Langmuir* **2010**, *26*, 17772−17779.
(56) Kuroda, K.; Ishida, T.; Haruta, M. *J. Mol. Catal. A: Chem.* **2009**, *298*, 7−11.
(57) Mahmoud, M. A.; El-Sayed, M. A. *Nano Lett.* **2011**, *11*, 946−953.
(58) Weng, G.; Mahmoud, M. A.; El-Sayed, M. A. *J. Phys. Chem. C* **2012**, *116*, 24171−24176.
(59) Deraedt, C.; Salmon, L.; Gatard, S.; Ciganda, R.; Hernandez, R.; Ruiz, J.; Astruc, D. *Chem. Commun.* **2014**, *50*, 14194−14196.
(60) Gómez-Lahoz, C.; García-Herruzo, F.; Rodríguez-Maroto, J. M.; Rodríguez, J. J. *Sep. Sci. Technol.* **1992**, *27*, 1449−1468.
(61) Li, M.; Chen, G.; Bhuyain, S. *Nanoscale* **2015**, *7*, 2641−2650.
(62) Mahmoud, M. A.; Garlyyev, B.; El-Sayed, M. A. *J. Phys. Chem. C* **2013**, *117*, 21886−21893.

DOI: 10.1021/acs.nanolett.6b03991
Nano Lett. 2016, 16, 7791−7797